İSTANBUL UNIVERSITY PRESS

INDUCED PLURIPOTENT STEM CELL-DERIVED MICROGLIA TO STUDY NLRP3 INFLAMMASOME ACTIVATION IN ALZHEIMER'S DISEASE

İNDÜKLENMİŞ PLURİPOTENT KÖK HÜCRE KAYNAKLI MİKROGLİA HÜCRELERİNİN ALZHEİMER HASTALIĞINDA NLRP3 İNFLAMAZOM AKTİVASYONU ARAŞTIRMALARINDA KULLANIMI

Aslı ERDOĞAN ÖNER[1,2] , Cira DANSOKHO[3] , Jari KOISTINAHO[4] , Sarka LEHTONEN[5] , Seyhun SOLAKOĞLU[1] , Michael T. HENEKA[6]

[1]İstanbul University, İstanbul Faculty of Medicine, Department of Histology and Embryology, İstanbul, Türkiye
[2]İzmir Katip Çelebi University, Faculty of Medicine, Department of Histology and Embryology, İzmir, Türkiye
[3]Evotec SE, Manfred Eugen Campus, Hamburg, Germany
[4]Neuroscience Center, HiLIFE, University of Helsinki, Helsinki, Finland
[5]A.I. Virtanen Institute for Molecular Sciences, University of Eastern Finland, Kuopio, Finland
[6]Luxembourg Centre for Systems Biomedicine, University of Luxembourg, Esch-Belval, Luxembourg

ORCID IDs of the authors: A.E.Ö. 0000-0002-7899-280X; C.D. 0000-0001-6868-0872; J.K. 0000-0001-6559-1153; S.L. 0000-0002-5055-9414; S.S. 0000-0002-1389-9639; M.T.H. 0000-0003-4996-1630

ABSTRACT

Objective: Alzheimer's disease (AD) is an irreversible and progressive neurodegenerative disease. Besides amyloid beta (Aβ) and tau accumulations, inflammation also contributes to AD pathogenesis. NLR family pyrin domain containing 3 (NLRP3) inflammasome activation in microglia is thought to be associated with AD. Since animal models of AD do not accurately reflect human pathology, in our study, human induced pluripotent stem cells (iPSCs) were differentiated into microglia, and their potential to be used in NLRP3 pathway-related mechanisms in AD was investigated.

Material and Method: iPSC cell lines of AD, isogenic, or control genotypes were differentiated into microglia and cells from different stages of the differentiation were characterized by flow cytometry, real-time quantitative polymerase chain reaction (RT-qPCR), immunocytochemistry, and Western blot. The expression of proteins associated with the NLRP3 pathway was investigated by Western blot. For functional analysis, cytokine release was assessed by Enzyme-linked immunosorbent assay (ELISA) upon NLRP3 inflammasome activators (lipopolysaccharide (LPS),

ÖZET

Amaç: Alzheimer hastalığı (AH) geri dönüşümsüz ve ilerleyici bir nörodejeneratif hastalıktır. Amiloid beta (Aβ) ve tau birikimlerinin yanı sıra, inflamasyon da AH patogenezinde rol oynamaktadır. Mikroglia hücrelerinde NLR ailesi pirin domain içeren 3 (NLRP3) inflamazomunun aktivasyonunun AH ile ilişkili olduğu düşünülmektedir. Hastalığın hayvan modelleri insandaki patolojiyi tam olarak yansıtamadığından, çalışmamızda insan kaynaklı indüklenmiş pluripotent kök hücreler (İPKH) mikrogliaya farklılaştırılarak, AH'de NLRP3 yolağı ilişkili mekanizmaların araştırılmasındaki kullanım potansiyeli incelenmiştir.

Gereç ve Yöntem: AH, izogenik ve kontrol genotipteki iPKH hücre hatları mikrogliaya farklılaştırılmış ve farklılaşmanın çeşitli aşamalarındaki hücreler akış sitometrisi, gerçek zamanlı kantitatif polimeraz zincir reaksiyonu (RT-qPCR), immünositokimya ve Western blot yöntemleriyle karakterize edilmiştir. NLRP3 yolağı ile ilişkili proteinlerin ekspresyonu Western blot ile incelenmiştir. Fonksiyonel analizler için, NLRP3 inflamazom aktivatörleri (lipopolisakkarid (LPS), Aβ) ve inhibitörü (sitokin salgılanmasını inhibe edici ilaç 3, CRID3) varlığında sitokin sa-

Aβ) and inhibitor (cytokine release inhibitory drug 3, CRID3) treatments. The phagocytosis of pHrodo particles and Aβ were evaluated by flow cytometry, fluorescence microscopy, and live cell imaging system.

Result: In our study, we could differentiate microglia from iPSCs derived from different genotypes. These microglia cells expressed various microglia and NLRP3 inflammasome-related markers and were able to phagocytose pHrodo particles and Aβ. The stimulation of the microglia cells with LPS and Aβ caused IL-1beta and IL-18 release, while CRID3 reversed this effect.

Conclusion: Our results show that iPSC-derived microglia generated in this study recapitulate microglia functional characteristics and can therefore be used to study NLRP3 pathway-associated disease mechanisms and treatment options.

Keywords: Microglia, induced pluripotent stem cells, neuroinflammation, NLRP3 inflammasome, amyloid beta

lımı ELISA ile ölçülmüştür. pHrodo partiküllerinin ve amiloid betanın fagositozu ise akış sitometrisi, floresan mikroskobu ve canlı hücre görüntüleme sistemi ile değerlendirilmiştir.

Bulgular: Çalışmamızda farklı genotiplerdeki İPKH'ler başarılı biçimde mikrogliaya farklılaştırılmıştır. Elde edilen mikroglia hücrelerinin çeşitli mikroglia ve NLRP3 inflamazomu ilişkili belirteçleri eksprese ettiği ve pHrodo ile amiloid betayı fagosite edebildiği gösterilmiştir. Mikroglia hücrelerinin LPS ve amiloid beta ile uyarılması IL-1beta ve IL-18 salımına neden olurken, CRID3 uygulanması bu etkiyi tersine çevirmiştir.

Sonuç: Çalışmamız İPKH'den farklılaştırılan mikroglia hücrelerinin, mikroglianın işlevsel özelliklerini taşıması nedeniyle NLRP3 yolağı ile ilişkili hastalık mekanizmalarının ve tedavi seçeneklerinin araştırılmasında kullanılabileceğini göstermektedir.

Anahtar Kelimeler: Mikroglia, indüklenmiş pluripotent kök hücreler, nöroinflamasyon, NLRP3 inflamazomu, amiloid beta

INTRODUCTION

Alzheimer's Disease (AD) is the leading cause of age-related dementia. It affects more than 50 million people worldwide (1). AD patients show progressive alterations of cognitive functions and have problems with communication, judgement, and orientation skills (2). Except for the limited number of drugs providing symptomatic treatment, there is no cure for AD (3).

The most prominent hallmarks of AD are the extracellular deposition of amyloid beta (Aβ) plaques and neurofibrillary tangles caused by the intracellular accumulation of hyperphosphorylated tau protein (4). Neuroinflammation, mediated by microglia and astrocytes surrounding Aβ plaques and neurofibrillary tangles, also contributes to the disease (5). Microglia, the innate immune cells of the central nervous system (CNS), plays a central role in brain homeostasis (6). They monitor the environment searching for pathogens and respond to inflammatory stimuli to maintain homeostasis (7). However, exposure to chronic stimuli causes microglial activation (8). Activated microglia switch to amoeboid morphology and have a number of changes such as surface markers and molecules that they release or recognize (7). They become more motile and migrate to the relevant area using chemotactic gradient clues (9).

Current studies have shown that the NLR family pyrin domain containing 3 (NLRP3) inflammasome pathway is activated in AD patients and mouse models (10, 11). NLRP3 is the best-characterized inflammasome consisting of NLRP3, apoptosis-associated speck-like protein containing a CARD (ASC), and caspase-1 proteins (12). The NLRP3 inflammasome pathway is activated in microglia in two steps. The first step is priming (e.g., triggered by lipopolysaccharide (LPS)), which promotes NF-kB gene transcription and pro-interleukin-1β (pro-IL-1β) and pro-IL-18 protein production, and the second step is activation (e.g., triggered by adenosine triphosphate (ATP), Aβ)

(13). The activation signal leads to the assembly of NLRP3 inflammasome components, promoting the cleavage of pro-caspase-1 to active caspase-1, which further induces the production of IL-1β and IL-18 in their mature form (14). Activation of this pathway in AD mouse model leads to increased Aβ deposition, reduced Aβ phagocytosis and results in cognitive impairment (11). Several studies have shown that NLRP3 inflammasome inhibition ameliorates Aβ pathology and protects against AD in rodent models (15, 16). Therefore, NLRP3 inflammasome inhibitors have been evaluated as therapeutic targets for AD. The cytokine release inhibitory drug 3 (CRID3) is one of the most potent and selective inhibitors of the NLRP3 inflammasome (17, 18). Inhibition of this pathway with CRID3 has been considered a promising anti-inflammatory therapy in AD (19).

Animal models have helped to investigate the key mechanisms involved in the physiopathology of AD. However, these models do not fully recapitulate the characteristics of AD and therefore need to be completed (20). The use of human-derived microglia is not always possible due to the inability to obtain samples from the CNS. The discovery of induced pluripotent stem cells (iPSCs) overcame the limited possibilities of animal models and offered a unique opportunity to investigate disease mechanisms using human-derived brain cells (21). Recently, several groups have proposed different methods to generate microglia from human iPSCs (22). As iPSCs represent the pathology better, they can be eligible to investigate new treatment opportunities in AD.

The aim of this study was to characterize human iPSC-derived microglia and investigate their potential to be used in NLRP3 pathway-related neuroinflammatory mechanisms involved in AD.

MATERIAL AND METHODS

Human iPSC cell lines

All three iPSC lines were reprogrammed from skin fibroblasts derived either from a control subject (CTL) or an AD

patient (AD) carrying the ΔE9 mutation in the presenilin-1 (*PSEN1*) gene. In addition, an isogenic line (ISO) was used where the mutation ΔE9 has been corrected in the AD line.

All the iPSC lines were generated with the approval of the committee on Research Ethics of Northern Savo Hospital district (Date: 29.04.2016, No: 123) after written consent from the subjects. iPSC lines were provided by the University of Eastern Finland (UEF) based on a material transfer agreement with the German Center for Neurodegenerative Diseases (DZNE).

iPSC-derived microglia cell culture

Microglial differentiation from iPSCs was performed according to a previously published protocol (23). iPSCs were expanded in mTeSR™ Plus medium (Stem Cell Technologies, Canada) on matrigel (Corning, USA). Firstly, hematopoietic progenitor cells (HPCs) were generated from iPSCs, and then they were differentiated into microglia (Figure 1A). All the cells were incubated under 37°C and 5% CO_2 conditions in an incubator (ICO 240, Memmert, Germany).

Flow cytometry analysis

Phenotypical characterization of the cells was performed using flow cytometry. For each sample $2x10^5$ cells were used. Fluorochrome-conjugated antibodies CD11b-BV605 (1:33 (v:v), 562721, Horizon, BD, USA), CD45-APC-Cy7 (1:33 (v:v), 557833, (Pharmingen, BD), CD200R-APC (1:33 (v:v), 329308, BioLegend, USA), P2RY12-PE (1:33 (v:v), 392104, BioLegend), CD14-PE-Cy7 (1:33 (v:v), 557742, Pharmingen, BD), CD16-BV421 (1:33 (v:v), 562874, Horizon, BD), CX3CR1-FITC (1:33 (v:v), 341606, BioLegend), CD235a-PE-Cy7 (1:33 (v:v), 349112, BioLegend), CD43-APC (1:33 (v:v), 343206, BioLegend), CD34-PE (1:33 (v:v), 130-120-515, Miltenyi Biotec, Germany) or primary antibodies anti-TMEM119 (1:50 (v:v), ab185333, Abcam, UK), anti-TREM2 (1:50 (v:v), MABN755, Millipore, French) followed by labelling with secondary antibodies goat anti-rabbit Alexa Fluor 647 (1:10000 (v:v), A-21244, Invitrogen, USA) or goat anti-rat Alexa Fluor 488 (1:10000 (v:v), A-11006, Invitrogen) were used. To assess cell viability, the cells were stained with 7-AAD (Pharmingen, BD). Samples were analyzed using a flow cytometer (FACS Canto II, BD), data were analyzed using FlowJo software (BD).

Real-Time quantitative PCR (RT-qPCR)

RNA purification was performed using the RNeasy® Mini Kit (74104, Qiagen, Germany). RNA concentration and purity were determined using a spectrophotometer (NanoDropTM 2000c, Thermo Scientific, USA). cDNAs were synthesized from RNA samples using the RT2 First Strand Kit (330404, Qiagen). PCR reaction was set using cDNAs, primers of related genes and RT2 SYBR® Green Master Mix (330502, Qiagen). Table 1 indicates information about the gene-specific primer assays (human) purchased (330001, RT2 qPCR Primer Assay, Qiagen). PCR conditions were determined as 1 cycle at 95°C for 10 min, 40 cycles at 95°C for 15 s and at 60°C for 1 min using a thermal cycler (StepOnePlus, Applied Biosystems, USA). Comparative Ct quantification (ΔΔCt method) was performed using glyceraldehyde 3-phosphate dehydrogenase (*GAPDH*) as the endogenous control gene, and relative fold changes were calculated comparing to control samples.

Table 1: Information about the primers used in the RT-qPCR assays (330001, RT2 qPCR Primer Assay, Qiagen)

| Gene symbol	Gene name	RefSeq accession number	Reference position
NANOG	Nanog homeobox	NM_024865	1774
SOX2	SRY (sex determining region Y)-box 2	NM_003106	1091
CD34	CD34 molecule	NM_001773	474
IBA1(AIF1)	Allograft inflammatory factor 1	NM_001623	349
CD14	CD14 molecule	NM_000591	463
CSF1	Colony-stimulating factor 1	NM_000757	738
CX3CR1	Chemokine (C-X3-C motif) receptor 1	NM_001337	558
TREM2	Triggering receptor expressed on myeloid cells 2	NM_018965	608
TLR2	Toll-like receptor 2	NM_003264	415
TLR4	Toll-like receptor 4	NM_138554	2695
P2RY12	Purinergic receptor P2Y, G-protein coupled, 12	NM_022788	1115
TUJ1 (TUBB3)	Tubulin, beta 3 class III	NM_006086	436
GFAP	Glial fibrillary acidic protein	NM_002055	1078
OLIG2	Oligodendrocyte lineage transcription factor 2	NM_005806	401
GAPDH	Glyceraldehyde-3-phosphate dehydrogenase	NM_002046	822
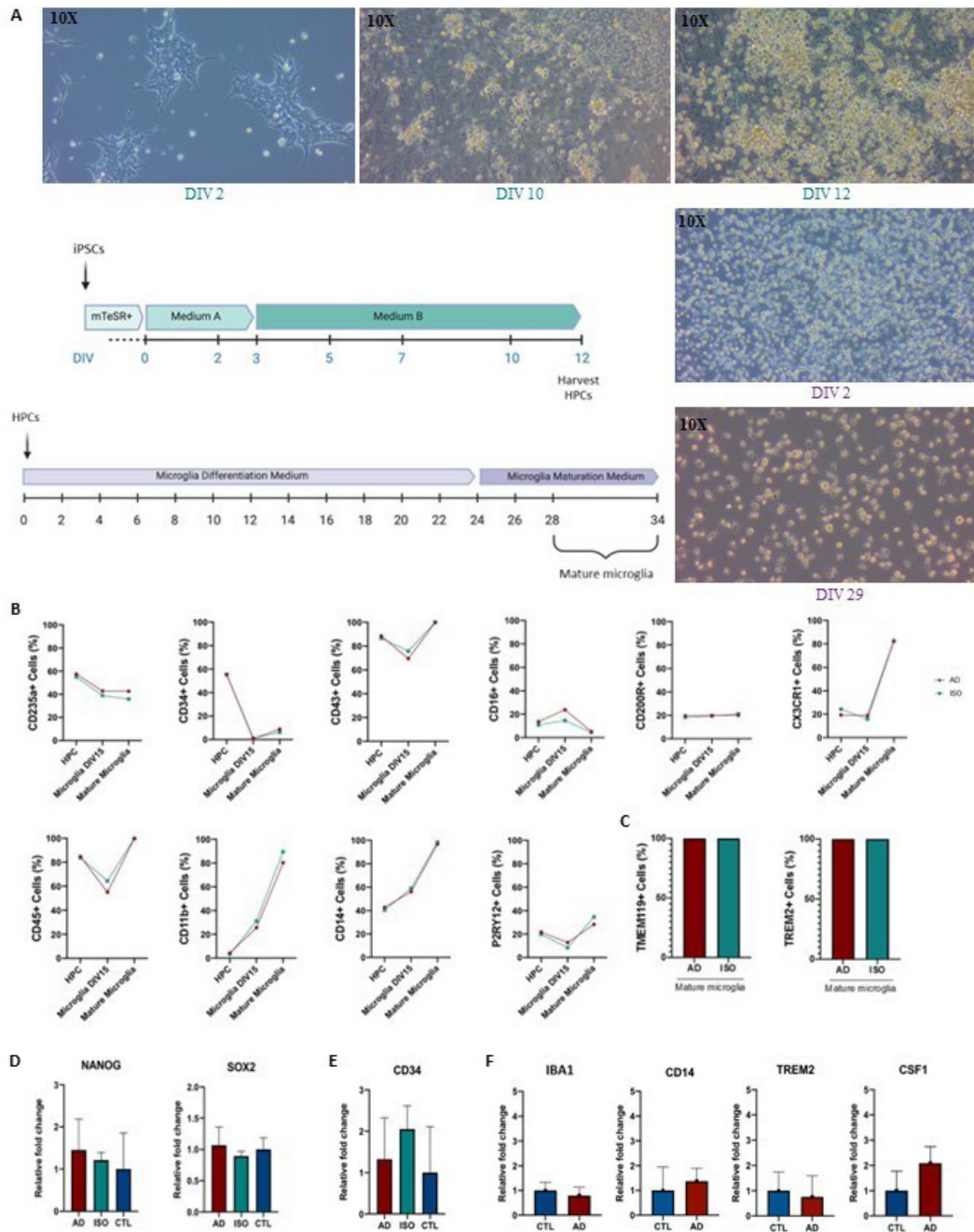
Figure 1:

Immunocytochemistry

Mature microglia were plated as 15×10^4 cells/well on PDL-coated 8-well chamber slide. Cells were fixed with 4% paraformaldehyde, permeabilized with 3% Triton X-100 in PBS, and blocked with 3% normal goat serum (Vector Laboratories, USA). Anti-TREM2 (1:500 (v:v), MABN755, Millipore), anti-IBA1 (1:250 (v:v), 019-19741, Wako, USA), anti-TMEM119 (1:500 (v:v), ab185333, Abcam) and anti-PU.1 (1:40 (v:v), PA5-35158, Thermo Fisher Scientific) primary antibodies, and goat anti-rabbit Alexa-Fluor 488 (1:10000 (v:v), A-11008, Invitrogen) or goat anti-rat Alexa-Fluor 488 (1:10000 (v:v), A-11006, Invitrogen) secondary antibodies were used. Cells were imaged using an Laser Confocal Scanning Microscope (LSM800, Zeiss, Germany) and images were processed using Image-J software (USA).
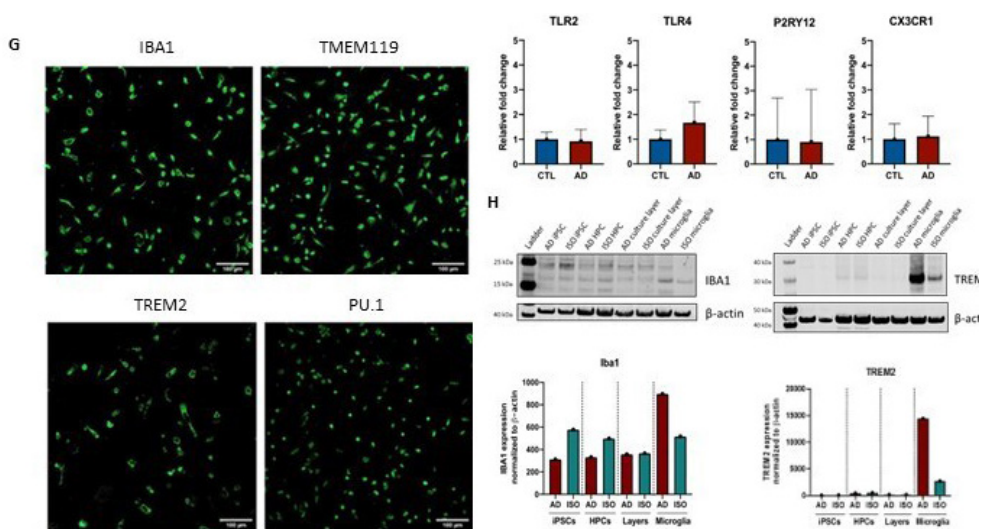
Figure 1: Continue. (A) A two-step protocol was used to obtain iPSC-derived microglia. In the first step of the protocol, HPCs were differentiated from iPSCs after 12 days. In the second step of the protocol, HPCs were driven into microglial differentiation for 24 days and after 4 days of further maturation, mature iPSC-derived microglia were obtained. (B, C) Percentages of positive cells analyzed by flow cytometry in HPCs, iPSC-derived microglia on day 15 (Microglia DIV15), and mature iPSC-derived microglia for CD235a, CD34, CD43, CD16, CD200R, CX3CR1, CD45, CD11b, CD14, P2RY12, TMEM119, and TREM2 markers (HPCs (n=3), Microglia DIV15 (n=3) and Mature Microglia (n=1)). Relative quantification of mRNA expressions of (D) pluripotency markers *NANOG* and *SOX2* in iPSCs, (E) hematopoietic marker *CD34* in HPCs, and (F) microglia-associated markers *IBA1, CD14, TREM2, CSF1, TLR2, TLR4, P2RY12,* and *CX3CR1* in iPSC-derived microglia by RT-qPCR. *GAPDH* was used as an endogenous control gene, and data are shown as fold increase relative to control samples. Experiments were carried out in triplicates. One-Way ANOVA, followed by Tukey's multiple-comparison post-hoc test (D, E) or unpaired Student's t-test (F). (G) Immunocytochemical staining of iPSC-derived microglia with IBA1, TMEM119, TREM2, and PU.1. Scale bar: 100 µm. (H) Western blots and quantification of the proteins IBA1 and TREM2 at different differentiation stages (iPSCs, HPCs, culture layers, and iPSC-derived microglia).

Western blot
Cells were lysed in RIPA lysis buffer, protein concentrations were determined using BCA Protein Assay Kit (Thermo Scientific). 20 µg proteins were separated on 4-12% Bis-Tris gels (Invitrogen) and blotted onto nitrocellulose membranes (Bio-Rad, USA) which were stained with anti-GSK3β (1:1000 (v:v), 9315, Cell Signaling Technology), anti-TUJ1 (1:1000 (v:v), MAB1195, R&D Systems, USA), anti-Nestin (1:2000 (v:v), PA5-11887, Thermo Fisher Scientific), anti-Olig-2 (1:500 (v:v), AV31464, Sigma-Aldrich, Germany), anti-ASC (1:1000 (v:v), AG-25B-0006-C100, Adipogen, USA), anti-NLRP3 (1:500 (v:v), AG-20B-0014-C100, Adipogen), anti-MyD88 (1:500 (v:v), ab2064, Abcam), anti-IBA1 (1:1000 (v:v), 17198, Cell Signaling Technology, USA), anti-TREM2 (1:1000 (v:v), ab209814, Abcam), anti-GFAP (1:1000 (v:v), MAB360, Millipore), anti-GAPDH (1:1000 (v:v), G9545, Sigma-Aldrich), anti-β-actin (1:1000 (v:v), MA5-15739, Thermo Fisher Scientific) antibodies and labelled with fluorescent near-infrared secondary antibodies IRDye 800CW Goat anti-rabbit IgG and IRDye 680LT Goat anti-mouse IgG (1:20000 (v:v), 926-32211 and 926-68020, LI-COR, USA). Proteins were visualized with an imaging system (Odyssey CLx Imaging System, LI-COR), images were analyzed using Image Studio (LI-COR). Protein levels were normalized to GAPDH or β-actin protein expressions.

Aβ preparation
Fibrillary Aβ Preparation: 1 mg HFIP (hexafluoro-2-propanol) treated Aβ$_{1-42}$ (Bachem, Switzerland) was dissolved in Dulbecco's Phosphate-Buffered Saline (DPBS) with 250 µM final concentration. Fibril formation was induced by incubating on a shaker at 1000 rpm and 37°C for 80 h, and the solution was kept at -80°C until use.

FAM-labelled Aβ Preparation: 0.5 mg fluorescently labelled Aβ$_{1-42}$ (AnaSpec, Eurogentec, USA) was dissolved in 40 mM NaOH and diluted to 221 µM with Tris HCl. After incubation at 37°C for 24 h, the solution was kept at -80°C until use.

Stimulation assays
Mature microglia were plated onto matrigel-coated plates and primed for 3 h with 100 ng/ml LPS (tlrl-eklps, InvivoGen, USA) and stimulated with 2,5 μM fibrillary Aβ for 24h. Cells were incubated in the presence or absence of 1 μM CRID3 (MCC950, Invivogen).

Measurement of cytokine secretion
Cytokines release after stimulation were measured by ELISA. Cell culture supernatants were assayed according to the manufacturer's protocol (human IL-1β, IL-18, IL-6,

CXCL12 DuoSet ELISA kit (R&D Systems)). Optical density was determined at 450 nm with a microplate reader (Infinite M200, Tecan, Switzerland), data were analyzed using GraphPad® Prism 8 software.

Phagocytosis analyses

Mature microglia were plated in Microglia Basal Medium on Matrigel-coated 24-well plates as 18×10^4 cells/well. After incubation with 10 µg/ml pHrodo bioparticles (Invitrogen) for 30 min, 1 h, and 2 h or 0.5 µM FAM-labelled Aβ (AnaSpec, Eurogentec) for 1 h, 3 h, and 5 h, the cells were collected from the plates and added in FACS tubes. The cells were stained with 7-AAD dye (Pharmingen, BD) for 10 min. Samples were analyzed using a BD FACSCanto II flow cytometer, data were analyzed using FlowJo software.

Live cell imaging

iPSC-derived microglia were plated in Microglia Differentiation Medium on PDL-coated 8-well chambers as 10^5 cells/well and incubated overnight. The medium was changed to Microglia Basal Medium and 40 µM TAMRA-labelled Aβ (AnaSpec, Eurogentec) was added. Timelapse images were taken during 1 h or 30 min, and videos were created from these images using Live Cell Imaging Microscopy (Eclipse Ti, Nikon, Japan) and NIS-Elements software (Nikon).

Statistical analyses

Graph Pad Prism software Version 8.0 was used. Statistical analysis was performed using one-way ANOVA or two-way ANOVA, followed by Tukey's multiple-comparison post hoc test or unpaired Student's t-test. Levels of significance were indicated as ****$p<0.0001$ ***$p<0.001$ **$p<0.01$ *$p<0.1$.

RESULTS

Characterization of iPSC-derived HPCs and microglia

iPSC-derived microglia were obtained at the end of 40 days of differentiation. In the first step, iPSCs were driven into mesodermal differentiation and then hematopoiesis was promoted. Round-shaped hematopoietic progenitor cells (HPCs) were obtained on day 12 (Figure 1A). In the second step, the collected HPCs were cultured in Microglia Differentiation Medium for 24 days. After four days of maturation in the Microglia Maturation Medium, iPSC-derived microglia were obtained (Figure 1A).

Flow cytometry showed that HPCs expressed hematopoietic markers CD43, CD235a, CD34 and also myeloid marker CD45 (Figure 1B). iPSC-derived microglia on day 15 started expressing CD11b and CD14 while hematopoietic marker expressions were decreasing. The expression of the myeloid markers CD45, CD11b, and CD14 was highly increased in mature microglia. Also, CX3CR1 and P2RY12 expressions increased when compared to HPCs. Almost all the cells of the mature microglia expressed the important microglia-associated markers TREM2 and TMEM119 (Figure 1C).

Various gene expressions of iPSC, HPC, and iPSC-derived microglia were determined by RT-qPCR. iPSCs expressed the pluripotency markers *NANOG* and *SOX2* (Figure 1D). HPCs expressed hematopoietic marker CD34 (Figure 1E), and iPSC-derived microglia expressed all the microglia-associated markers that were tested (Figure 1F).

Immunocytochemistry for IBA1, TMEM119, TREM2, and PU.1 was performed. iPSC-derived microglia were positively stained with all four markers (Figure 1G).

IBA1 and TREM2 expressions during differentiation were also analyzed by Western blot. IBA1 was slightly expressed in all stages of differentiation, but its expression was increased in iPSC-derived microglia, especially in the AD genotype (Figure 1H). TREM2 was only expressed in iPSC-derived microglia (Figure 1H). IBA1 and TREM2 proteins were expressed higher in the AD genotype compared to ISO.

Characterization of culture layers

During differentiation, iPSCs formed a layer of attached cells, which we named culture layer, and on top of which HPCs pop off (Figure 2A). We aimed to characterize culture layers after collecting the HPCs. Western blot results revealed that TUJ-1 was highly expressed in the culture layers of all genotypes (Figure 2B). However, a very low level to no expression of GFAP was detected (Figure 2B). In addition, neural progenitor cell (NESTIN) and oligodendrocyte (OLIG-2) markers were not detected in the culture layers by Western blot (not shown).

TUJ1, GFAP, and OLIG-2 expressions of the culture layers were also assessed by RT-qPCR, and similar results were obtained. TUJ1 was highly expressed in the culture layers (Figure 2C). However, GFAP and OLIG-2 expressions were not detected (not shown).

Aβ caused NLRP3-related cytokines release in iPSC-derived microglia

iPSC-derived microglia expressed ASC and NLRP3 proteins, but very low/no expression was detected in iPSC, HPC, and culture layers (Figure 3A). MyD88 protein was expressed in iPSC, culture layer, and iPSC-derived microglia at low levels, but no expression was detected in HPC samples (Figure 3A). GSK3β protein was prominently expressed in iPSC, the culture layer, and iPSC-derived microglia, but no expression was detected in the HPC samples (Figure 3A).

To characterize NLRP3 inflammasome pathway activation, ELISA analyses were performed after the stimulation assays (Figure 3B). Aβ stimulation after LPS priming caused a significant increase in IL-1β and IL-18 release (Figure 3C). In the presence of CRID3, this effect was counteract-
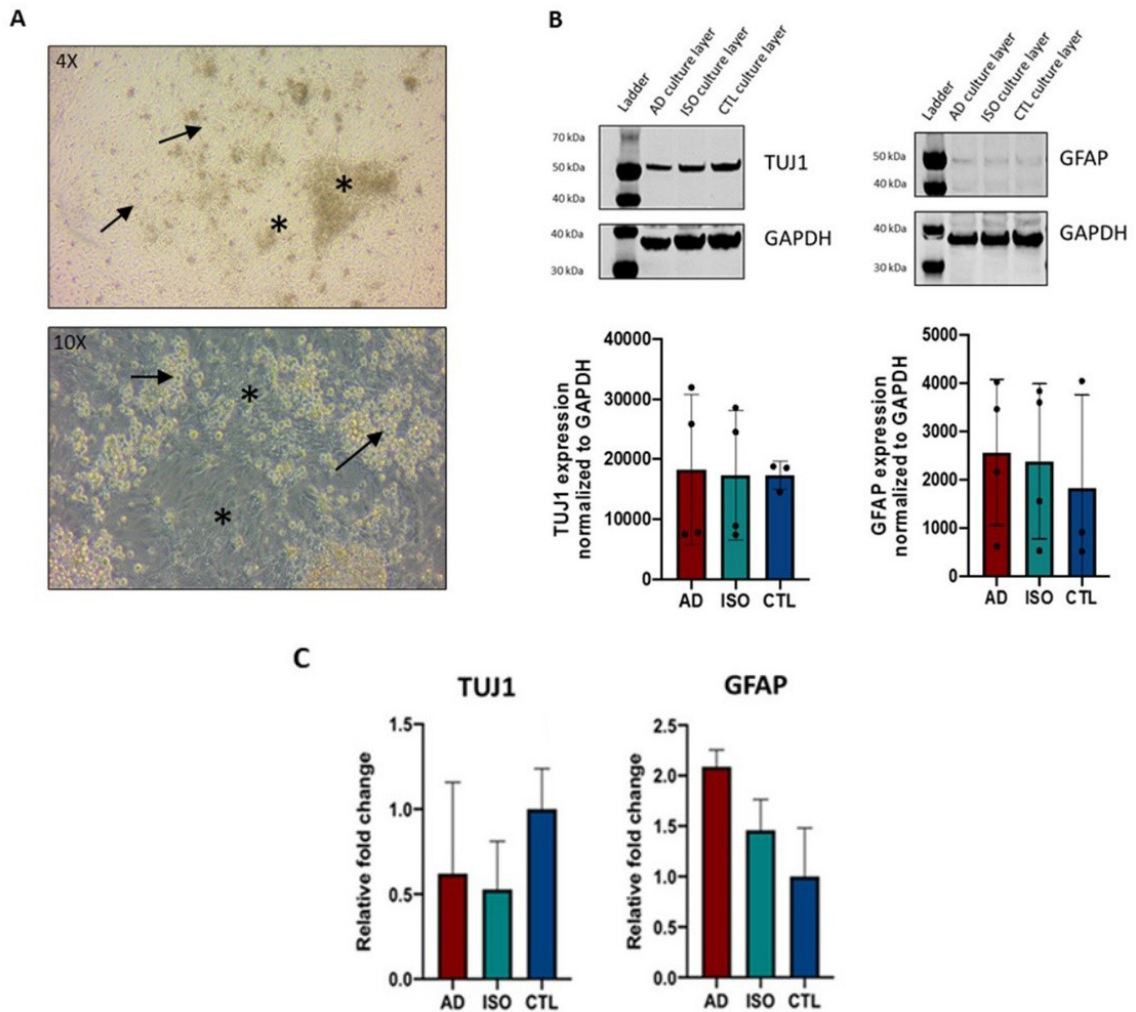
Figure 2: (A) During differentiation, iPSCs form a layer of attached cells called the culture layer (asterisks), on top of which HPCs (arrows) pop off. (B) Western blots and quantification for the proteins TUJ1 and GFAP of the culture layers (n=4). (C) Relative quantification of mRNA expressions of *TUJ1* and *GFAP* in the culture layers by RT-qPCR. *GAPDH* was used as an endogenous control gene, and data are shown as fold increase relative to the control samples. Experiments were carried out in triplicates. One-Way ANOVA, followed by Tukey's multiple comparison post hoc test.

ed. The secretions of other pro-inflammatory cytokines were also measured. LPS priming and Aβ stimulation after LPS priming increased IL-6 release, but this increase was not statistically significant (Figure 3C). Aβ stimulation after LPS priming caused an increase in CXCL12 release, and CRID3 treatment decreased this release (Figure 3C).

iPSC-derived microglia phagocytosed pHrodo bioparticles and Aβ

The phagocytosis of pHrodo bioparticles by iPSC-derived microglia was increased in a time-dependent manner (Figure 4A). Phagocytosis of pHrodo bioparticles were visualized using fluorescence microscopy (Figure 4B).

The percentages of Aβ phagocytosis by iPSC-derived microglia were high for both genotypes. (Figure 4C). iP-

SC-derived microglia of the AD genotype were observed to be slightly more phagocytic than those of the ISO genotype, but this difference was not statistically significant.

Aβ phagocytosis of the cells was also observed with live-cell imaging. iPSC-derived microglia of the AD genotype were observed to be more phagocytic than those of the ISO genotype (Figure 4D).

DISCUSSION

Recent studies have revealed the importance of neuroinflammation in AD and highlighted the role of microglia as one of the main regulators of neuroinflammation (24). Until recently, microglia studies were limited to animal models, biopsy of patients, or post-mortem brain samples (25). Although animal models have provided us with
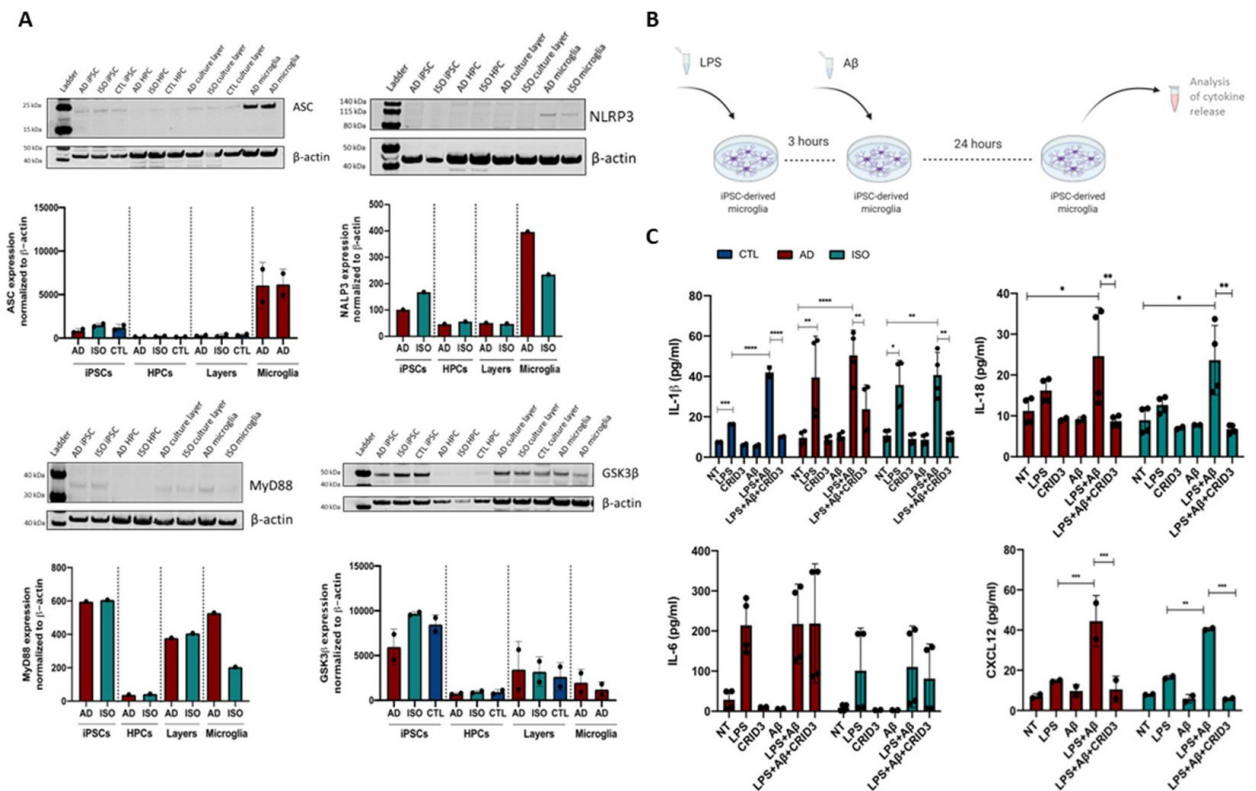
Figure 3: (A) Western blots and quantification for the proteins ASC, NLRP3, MYD88, and GSK3β of different differentiation stages (iPSCs, HPCs, culture layers, and iPSC-derived microglia); ASC and GSK3β (n=2), NLRP3 and MYD88 (n=1). (B) Scheme of stimulation experiments showing 3 h LPS priming and 24 hours Aβ stimulation of iPSC-derived microglia. (C) IL-1β, IL-18, IL-6, and CXCL12 release of iPSC-derived microglia upon LPS priming and Aβ stimulation in the presence or absence of CRID3. Experiments were carried out in duplicates (except CXCL12; n=1). Two-Way ANOVA, followed by Tukey's multiple-comparison post hoc test, *:p<0.1, **:p<0.01, ***:p<0.001, ****:p<0.0001.

very useful information regarding the pathogenesis of AD, failures in drug development studies have led to the questioning of these models. Since the etiology of AD is still not fully known, the ability of many proposed AD animal models to represent AD pathology is limited. For example, although animal models produced by the over-expression of AD-related genes recapitulate Aβ plaques, neuroinflammation, and memory loss, they fail to display neuronal death and degeneration, which are important hallmarks of AD in humans. Additionally, transcriptomic studies demonstrated substantial differences between murine and human microglia, including different aging. Most animal models fail to demonstrate the molecular signatures implicated in human AD cases, such as neuroinflammatory responses, antigen presentation, and adaptive immune responses (20, 26). Since the accessibility of human brain tissue is very limited, the number of studies on primary human microglia is few and restricted to patient samples or post-mortem tissue harvesting. Working with these samples brings problems, such as limited number of cells, post-mortem artefacts, and lack of healthy controls. Since iPSCs can be obtained from both patients and healthy individuals, provide a physio-

logically relevant background, can be proliferated indefinitely, and can be differentiated into desired brain cells, they present a valuable human cell source for investigating AD mechanisms by overcoming the limitations of the previous models (22).

Microglia originate from mesodermal primitive yolk sac progenitors, which give rise to erythromyeloid progenitors (EMPs) (27, 28). EMPs form yolk sac macrophages at E17 and migrate to the brain to form microglia from E31 until the blood-brain barrier is closed. Microglia that interact with other brain cells become mature and functional (22, 29). By mimicking the developmental stages, research groups have developed protocols to differentiate iPSCs into microglia. Although the basic approach is the same, each protocol has differences. As the first step of differentiation, iPSCs were directed to mesodermal differentiation using growth factors, and myeloid progenitors/erythro-myeloid progenitors were obtained. Afterwards, the cells were supported with essential growth factors and signaling molecules to promote microglial differentiation. For maturation, microglia co-cultured with neurons/astrocytes or maturation factors (CD200 and CX3CL1) were added to
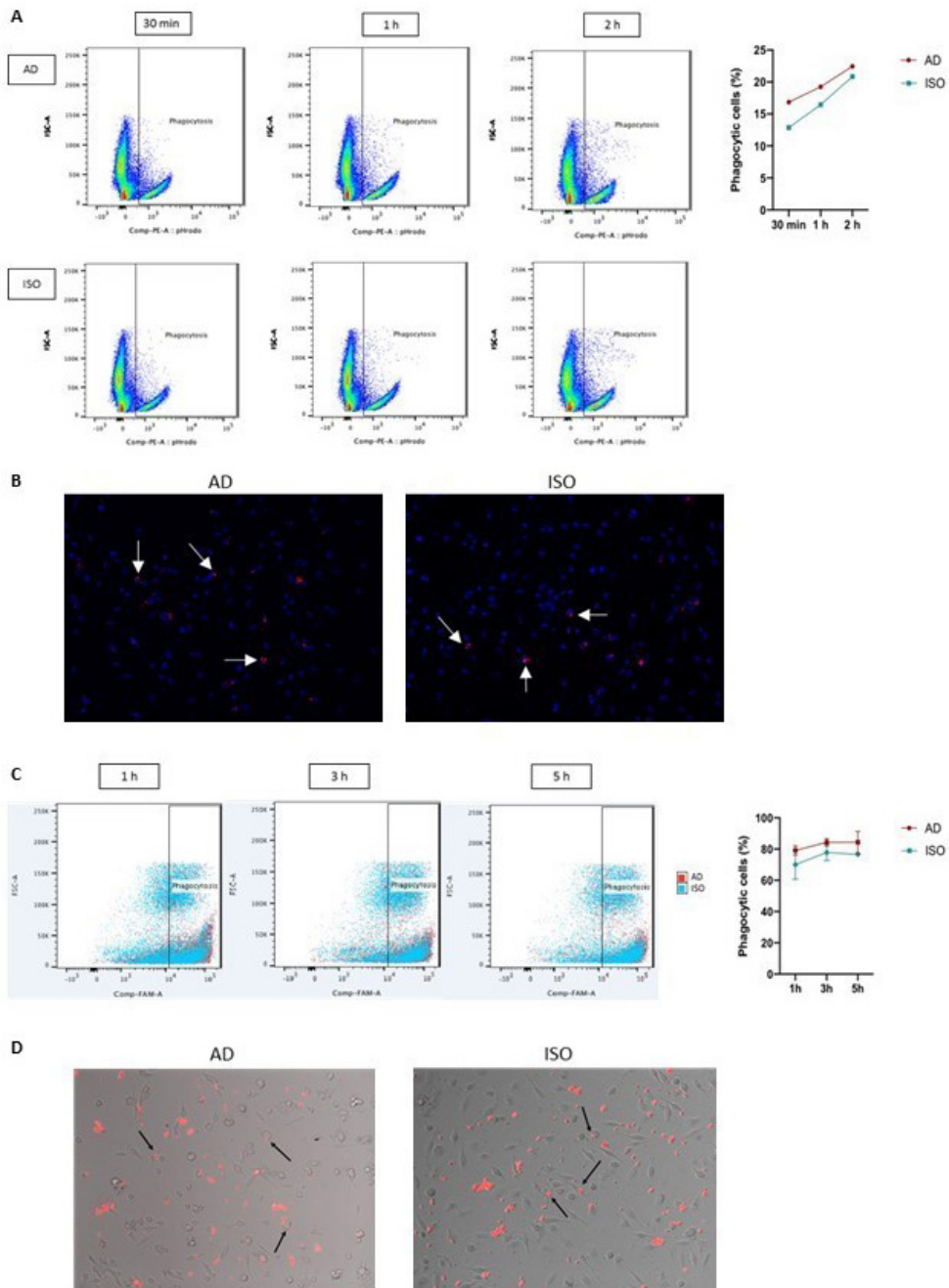
Figure 4: (A) Flow cytometry graphs showing pHrodo phagocytosis of iPSC-derived microglia after 30 min, 1 h, and 2 h incubation with pHrodo bioparticles (n=1). (B) Fluorescence microscopy images of iPSC-derived microglia showing nuclei of the cells (blue) and phagocytosed pHrodo bioparticles (red, arrows), 20X. (C) Flow cytometry graphs showing Aβ phagocytosis of iPSC-derived microglia after 1 h, 3 h, and 5 h incubation with FAM-labelled Aβ, (n=2). Two-Way ANOVA, followed by Tukey's multiple-comparison post-hoc test. (D) Live cell imaging microscopy photographs showing TAMRA-labelled Aβ phagocytosis (arrows) of iPSC-derived microglia, 20X.

the media (23, 29-31). Some methods required low oxygen conditions or the separation of cells by FACS using specific markers (30-34). As McQuade et al. suggested a simplified method that does not need hypoxic incubation, FACS sorting, or co-culture, we followed their protocol to obtain microglia from iPSCs (23).

Following the protocol, during mesodermal differentiation, iPSCs formed an attached layer of an unknown cell population, which we call culture layer, on top of which HPCs pop off. After collecting HPCs as a suspension on day 12, analysis of the culture layers revealed the expression of the neuronal marker TUJ-1 both at the mRNA and protein levels. Foudah et al. reported the spontaneous expression of neural markers, including TUJ-1, in undifferentiated mesenchymal stem cells from different sources (35). However, Bianchi et al. showed that undifferentiated iPSC colonies did not express TUJ-1 (36). TUJ-1 is known as an early neuronal marker widely used in stem cell studies to verify neuronal differentiation. In this context, TUJ-1 expression in the culture layers indicates that, although not targeted, neuronal differentiation of iPSCs may have been induced in the culture layers, and neurons may be the main supportive cells of microglial differentiation in this protocol.

One of the challenging problems of microglia research is that there is no specific marker for microglia. Some highly used common microglia markers (CD45, CD11b, IBA1) are known to be shared with other cell types like macrophages. Therefore, several studies have proposed potential markers specific to microglia. To the current knowledge, TREM2, TMEM119, CX3CR1, and P2RY12 are considered as the most specific microglia markers in human tissues (37, 38). TREM2 is involved in processes such as phagocytosis, proliferation, and chemotaxis, is a marker of tissue-specific macrophages, and is known to be expressed only by microglia in the brain. Garcia-Reitboeck et al. showed TREM2 expression in microglia differentiated from human iPSCs (39). TMEM119 is a transmembrane protein originally described as a regulator of osteoblast differentiation. Transcriptomic studies have shown that TMEM119 is expressed specifically by microglia in the CNS (40). Subsequent studies suggested TMEM119 to distinguish microglia from blood-derived macrophages infiltrating the CNS (41). CX3CR1, a chemokine receptor expressed in microglia, is involved in the recruitment of mononuclear phagocytes to the inflammation site. Since neurons express CX3CL1, the ligand of the receptor, CX3CR1-CX3CL1 signaling pathway plays an important role in microglia and neuron communication (42). P2RY12, a purinergic receptor located on the surface of microglia, detects molecules such as ATP released from damaged cells in case of danger and is involved in processes related to inflammation, cell movement and cell migration (43). In this study, we have validated that iPSC-derived microglia express the microglia-specific markers TREM2, TMEM119, CX3CR1, and P2RY12 in addition to the common microglia markers.

Microglia are responsive to inflammatory stimuli, and an exaggerated inflammatory response is involved in AD (38). Several studies have shown that inhibition of the NLRP3 inflammasome pathway improves amyloid pathology in rodent disease models and may be protective against AD (15, 16). Therefore, NLRP3 inflammasome inhibitors are considered among the therapeutic targets. CRID3 is one of the most effective and selective inhibitors of the NLRP3 inflammasome. It binds to the Walker B motif in the NACHT domain of the NLRP3 protein and puts it in a more closed and inactive conformation. This prevents ATP hydrolysis of NLRP3, thus preventing the activation of the NLRP3 inflammasome (18). Lučiūnaitė et al. showed that increased IL-1β levels upon stimulation with Aβ after LPS priming decreased after CRID3 administration in primary mouse microglia (44). Dempsey et al. stated that Aβ pathology was reduced and IL-1β level was decreased in brain homogenates upon CRID3 treatment in APP/PS1 mice (45). Mouton-Liger et al. showed that increased levels of IL-1β and IL-18 with NLRP3 activators were decreased with CRID3 treatment in primary mouse microglia (46). Clénet et al. differentiated microglia from iPSCs of Amyotrophic Lateral Sclerosis patients and healthy subjects (47). LPS treatment caused increase of IL-1β level, while CRID3 decreased this effect. In our study, we showed that iPSC-derived microglia expressed NLRP3 pathway-related proteins, and stimulation with Aβ after LPS priming resulted in the release of IL-1β and IL-18 cytokines. Moreover, in the presence of CRID3, cytokine releases were significantly reduced. Our results indicate that iPSC-derived microglia do not only express microglial markers but also show critical functional microglial features like being responsive to important stimulators in AD. Also, together with previous research, our results support that inhibition of the NLRP3 inflammasome pathway using inhibitors such as CRID3 can be evaluated as a new anti-inflammatory treatment method for AD.

Microglia recognize and phagocytose foreign particles and protein aggregates via various receptors on their surface. Our study showed that iPSC-derived microglia can successfully phagocyte pHrodo and Aβ. These data indicate that iPSC-derived microglia do not only express microglia-associated markers but also carry the phagocytic function of microglia. One of the proposed mechanisms of AD is the inability of microglia to clear Aβ deposits due to decreased phagocytic activity. However, there are controversial results regarding microglial phagocytosis in AD. In 5XFAD mice, microglia around Aβ plaques took up Aβ which is followed by microglial cell death, and dying microglia released Aβ deposits in the extracellular space, contributing to Aβ plaque growth (48). In APP/PS1 mice, deficiency of TAM receptors that function in Aβ phagocytosis of microglia resulted in fewer dense core plaques, showing that phagocytosis does not prevent the development of Aβ plaques, but rather promotes it (49). Xu et al. stated that human iPSC-derived microglia-like cells (iMGL) originating from sporadic AD lines showed higher phagocytic ability than control lines (50). However, Konttinen et al. reported dampening of phagocytosis in APOE4 iMGLs, but no change in APPswe or PSEN1ΔE9 iMGLs (33). In our study, we evaluated pHrodo and Aβ phagocytosis ability

of iPSC-derived microglia and the AD genotype seemed more phagocytic than that of the ISO genotype. Further research is needed to elucidate whether microglial phagocytosis contributes to the disease pathology in AD.

CONCLUSION

In summary, our study shows that iPSC-derived microglia provide key phenotypical and functional characteristics of microglia, such as expressing various distinctive microglial markers, being responsive to stimulant molecules, and being able to phagocytose Aβ. As iPSC-derived microglia originate from patients' own cells, this helps to overcome the limitations of AD studies related to animal models. Our results support that human iPSC-derived microglia can be a critical tool for understanding human AD pathogenesis, identifying therapeutic targets, and allowing large-scale drug screening of novel therapeutic candidates related to the NLRP3 inflammasome pathway.

REFERENCES

1. Li T, Lu L, Pember E, Li X, Zhang B, Zhu Z. New Insights into neuroinflammation involved in pathogenic mechanism of Alzheimer's disease and its potential for therapeutic intervention. Cells 2022;11:1925. [CrossRef]
2. 2022 Alzheimer's disease facts and figures. Alzheimer's and Dementia 2022;18(4):700-89. [CrossRef]
3. McManus RM. The Role of Immunity in Alzheimer's Disease. Adv Biol 2022;6(5):2101166. [CrossRef]
4. Crews L, Masliah E. Molecular mechanisms of neurodegeneration in Alzheimer's disease. Hum Mol Genet 2010;19(R1):R12-20. [CrossRef]
5. Heneka MT, Carson MJ, Khoury J El, Landreth GE, Brosseron F, Feinstein DL, et al. Neuroinflammation in Alzheimer's disease. Lancet Neurol 2015;14(4):388-405. [CrossRef]
6. Heppner FL, Ransohoff RM, Becher B. Immune attack: The role of inflammation in Alzheimer disease. Nat Rev Neurosci 2015;16(6):358-72. [CrossRef]
7. Li JW, Zong Y, Cao XP, Tan L, Tan L. Microglial priming in Alzheimer's disease. Ann Transl Med 2018;6(10):176. [CrossRef]
8. Kettenmann H, Hanisch UK, Noda M, Verkhratsky A. Physiology of microglia. Physiol Rev 2011;91(2):461-553. [CrossRef]
9. Fan Y, Xie L, Chung CY. Signaling pathways controlling microglia chemotaxis. Mol Cells 2017;40(3):163-8. [CrossRef]
10. Heneka MT, Kummer MP, Stutz A, Delekate A, Schwartz S, Vieira-Saecker A, et al. NLRP3 is activated in Alzheimer's disease and contributes to pathology in APP/PS1 mice. Nature 2013;493(7434):674-8. [CrossRef]
11. Rui W, Xiao H, Fan Y, Ma Z, Xiao M, Li S, et al. Systemic inflammasome activation and pyroptosis associate with the progression of amnestic mild cognitive impairment and Alzheimer's disease. J Neuroinflammation 2021;18(1):280. [CrossRef]
12. Dansokho C, Heneka MT. Neuroinflammatory responses in Alzheimer's disease. J Neural Transm 2018;125(5):771-9. [CrossRef]
13. Swanson K, Deng M, Ting JPY. The NLRP3 inflammasome: molecular activation and regulation to therapeutics. Nat Rev Immunol 2019;19:477-89. [CrossRef]
14. Liang T, Zhang Y, Wu S, Chen Q, Wang L. The Role of NLRP3 Inflammasome in Alzheimer's Disease and Potential Therapeutic Targets. Front Pharmacol 2013;13:845185. [CrossRef]
15. Daniels MJD, Rivers-Auty J, Schilling T, Spencer NG, Watremez W, Fasolino V, et al. Fenamate NSAIDs inhibit the NLRP3 inflammasome and protect against Alzheimer's disease in rodent models. Nat Commun 2016;7:12504. [CrossRef]
16. Yin J, Zhao F, Chojnacki JE, Fulp J, Klein WL, Zhang S, et al. NLRP3 inflammasome inhibitor ameliorates amyloid pathology in a mouse model of Alzheimer's disease. Mol Neurobiol 2018;55(3):1977-87. [CrossRef]
17. Zahid A, Li B, Kombe AJK, Jin T, Tao J. Pharmacological inhibitors of the NLRP3 inflammasome. Front Immunol 2019;10:2538. [CrossRef]
18. Coll RC, Hill JR, Day CJ, Zamoshnikova A, Boucher D, Massey NL, et al. MCC950 directly targets the NLRP3 ATP-hydrolysis motif for inflammasome inhibition. Nat Chem Biol 2019;15(6):556-9. [CrossRef]
19. Barczuk J, Siwecka N, Lusa W, Rozpędek-Kamińska W, Kucharska E, Majsterek I. Targeting NLRP3-Mediated Neuroinflammation in Alzheimer's Disease Treatment. Int Journal of Mol Sci 2022;23(16):8979. [CrossRef]
20. Galatro TF, Holtman IR, Lerario AM, Vainchtein ID, Brouwer N, Sola PR, et al. Transcriptomic analysis of purified human cortical microglia reveals age-associated changes. Nat Neurosci 2017;20(8):1162-71. [CrossRef]
21. Washer SJ, Perez-Alcantara M, Chen Y, Steer J, James WS, Trynka G, et al. Single-cell transcriptomics defines an improved, validated monoculture protocol for differentiation of human iPSC to microglia. Sci Rep 2022;12(1):19454. [CrossRef]
22. Hasselmann J, Blurton-Jones M. Human iPSC-derived microglia: A growing toolset to study the brain's innate immune cells. Glia 2020;68(4):721-39. [CrossRef]

23. McQuade A, Coburn M, Tu CH, Hasselmann J, Davtyan H, Blurton-Jones M. Development and validation of a simplified method to generate human microglia from pluripotent stem cells. Mol Neurodegener 2018;13:67. [CrossRef]

24. Leng F, Edison P. Neuroinflammation and microglial activation in Alzheimer disease: where do we go from here? Nat Rev Neurol 2021;17:157-72. [CrossRef]

25. Pocock JM, Piers TM. Modelling microglial function with induced pluripotent stem cells: An update. Nat Rev Neurosci 2018;19(8):445-52. [CrossRef]

26. Friedman BA, Srinivasan K, Ayalon G, Meilandt WJ, Lin H, Huntley MA, et al. Diverse brain myeloid expression profiles reveal distinct microglial activation states and aspects of Alzheimer's disease not evident in mouse models. Cell Rep 2018;22(3):832-47. [CrossRef]

27. Kierdorf K, Erny D, Goldmann T, Sander V, Schulz C, Perdiguero EG, et al. Microglia emerge from erythromyeloid precursors via Pu.1-and Irf8-dependent pathways. Nat Neurosci 2013;16(3):273-80. [CrossRef]

28. Ginhoux F, Greter M, Leboeuf M, Nandi S, See P, Gokhan S, et al. Fate mapping analysis reveals that adult microglia derive from primitive macrophages. Science 2010;330(6005):841-5. [CrossRef]

29. Haenseler W, Sansom SN, Buchrieser J, Newey SE, Moore CS, Nicholls FJ, et al. A Highly Efficient Human Pluripotent Stem Cell Microglia Model Displays a Neuronal-Co-culture-Specific Expression Profile and Inflammatory Response. Stem Cell Rep 2017;8(6):1727-42. [CrossRef]

30. Pandya H, Shen MJ, Ichikawa DM, Sedlock AB, Choi Y, Johnson KR, et al. Differentiation of human and murine induced pluripotent stem cells to microglia-like cells. Nat Neurosci 2017;20(5):753-9. [CrossRef]

31. Takata K, Kozaki T, Lee CZW, Thion MS, Otsuka M, Lim S, et al. Induced-Pluripotent-Stem-Cell-Derived Primitive Macrophages Provide a Platform for Modeling Tissue-Resident Macrophage Differentiation and Function. Immunity 2017;47(1):183-98. [CrossRef]

32. Abud EM, Ramirez RN, Martinez ES, Healy LM, Nguyen CHH, Newman SA, et al. iPSC-derived human microglia-like cells to study neurological diseases. Neuron 2017;94(2):278-93. [CrossRef]

33. Konttinen H, Cabral-da-Silva M e. C, Ohtonen S, Wojciechowski S, Shakirzyanova A, Caligola S, et al. PSEN1ΔE9, APPswe, and APOE4 Confer Disparate Phenotypes in Human iPSC-Derived Microglia. Stem Cell Rep 2019;13(4):669-83. [CrossRef]

34. Douvaras P, Sun B, Wang M, Kruglikov I, Lallos G, Zimmer M, et al. Directed Differentiation of Human Pluripotent Stem Cells to Microglia. Stem Cell Rep 2017;8(6):1516-24. [CrossRef]

35. Foudah D, Monfrini M, Donzelli E, Niada S, Brini AT, Orciani M, et al. Expression of neural markers by undifferentiated mesenchymal-like stem cells from different sources. J Immunol Res 2014;2014:987678. [CrossRef]

36. Bianchi F, Malboubi M, Li Y, George JH, Jerusalem A, Szele F, et al. Rapid and efficient differentiation of functional motor neurons from human iPSC for neural injury modelling. Stem Cell Res 2018;32:126-34. [CrossRef]

37. Böttcher C, Schlickeiser S, Sneeboer MAM, Kunkel D, Knop A, Paza E, et al. Human microglia regional heterogeneity and phenotypes determined by multiplexed single-cell mass cytometry. Nat Neurosci 2019;22(1):78-90. [CrossRef]

38. Melief J, Sneeboer MAM, Litjens M, Ormel PR, Palmen SJMC, Huitinga I, et al. Characterizing primary human microglia: A comparative study with myeloid subsets and culture models. Glia 2016;64(11):1857-68. [CrossRef]

39. Garcia-Reitboeck P, Phillips A, Piers TM, Villegas-Llerena C, Butler M, Mallach A, et al. Human Induced Pluripotent Stem Cell-Derived Microglia-Like Cells Harboring TREM2 Missense Mutations Show Specific Deficits in Phagocytosis. Cell Rep 2018;24(9):2300-11. [CrossRef]

40. Satoh J, Kino Y, Asahina N, Takitani M, Miyoshi J, Ishida T, et al. TMEM119 marks a subset of microglia in the human brain. Neuropathology 2016;36(1):39-49. [CrossRef]

41. Bohnert S, Seiffert A, Trella S, Bohnert M, Distel L, Ondruschka B, et al. TMEM119 as a specific marker of microglia reaction in traumatic brain injury in postmortem examination. Int J Legal Med 2020;134(6):2167-76. [CrossRef]

42. Murai N, Mitalipova M, Jaenisch, R. Functional analysis of CX3CR1 in human induced pluripotent stem (iPS) cell-derived microglia-like cells. Eur J Neurosci 2020;52(7):3667-78. [CrossRef]

43. Morillas AG, Besson VC, Lerouet D. Microglia and neuroinflammation: What place for p2ry12? Int J Mol Sci 2021;22(4):1-16. [CrossRef]

44. Lučiūnaitė A, McManus RM, Jankunec M, Rácz I, Dansokho C, Dalgėdienė I, et al. Soluble Aβ oligomers and protofibrils induce NLRP3 inflammasome activation in microglia. J Neurochem 2020;155(6):650-61. [CrossRef]

45. Dempsey C, Rubio Araiz A, Bryson KJ, Finucane O, Larkin C, Mills EL, et al. Inhibiting the NLRP3 inflammasome with MCC950 promotes non-phlogistic clearance of amyloid-β and cognitive function in APP/PS1 mice. Brain Behav Immun 2017;61:306-16. [CrossRef]

46. Mouton-Liger F, Rosazza T, Sepulveda-Diaz J, Ieang A, Hassoun SM, Claire E, et al. Parkin deficiency modulates NLRP3 inflammasome activation by attenuating an A20-dependent negative feedback loop. Glia 2018;66(8):1736-51. [CrossRef]

47. Clénet ML, Keaney J, Gillet G, Valadas JS, Langlois J, Cardenas A, et al. Divergent functional outcomes of NLRP3 blockade downstream of multi-inflammasome activation: therapeutic implications for ALS. Front Immunol 2023;14:1190219. [CrossRef]

48. Baik SH, Kang S, Son SM, Mook-Jung I. Microglia contributes to plaque growth by cell death due to uptake of amyloid β in the brain of Alzheimer's disease mouse model. Glia 2016;64(12):2274-90. [CrossRef]

49. Huang Y, Happonen KE, Burrola PG, O'Connor C, Hah N, Huang L, et al. Microglia use TAM receptors to detect and engulf amyloid β plaques. Nat Immunol 2021;22(5):586-94. [CrossRef]

50. Xu M, Zhang L, Liu G, Jiang N, Zhou W, Zhang Y. Pathological Changes in Alzheimer's Disease Analyzed Using Induced Pluripotent Stem Cell-Derived Human Microglia-Like Cells. J Alzheimer's Dis 2019;67(1):357-68. [CrossRef]